vol. 169, no. 1 the american naturalist january 2007

E-Article

Habitat Connectivity and Ecosystem Productivity: Implications from a Simple Model

James E. Cloern*

U.S. Geological Survey, Menlo Park, California 94025

Submitted December 1, 2005; Accepted August 10, 2006; Electronically published December 4, 2006

abstract: The import of resources (food, nutrients) sustains biological production and food webs in resource-limited habitats. Resource export from donor habitats subsidizes production in recipient habitats, but the ecosystem-scale consequences of resource translocation are generally unknown. Here, I use a nutrient-phytoplankton-zooplankton model to show how dispersive connectivity between a shallow autotrophic habitat and a deep heterotrophic pelagic habitat can amplify overall system production in metazoan food webs. This result derives from the finite capacity of suspension feeders to capture and assimilate food particles: excess primary production in closed autotrophic habitats cannot be assimilated by consumers; however, if excess phytoplankton production is exported to food-limited heterotrophic habitats, it can be assimilated by zooplankton to support additional secondary production. Transport of regenerated nutrients from heterotrophic to autotrophic habitats sustains higher system primary production. These simulation results imply that the ecosystem-scale efficiency of nutrient transformation into metazoan biomass can be constrained by the rate of resource exchange across habitats and that it is optimized when the transport rate matches the growth rate of primary producers. Slower transport (i.e., reduced connectivity) leads to nutrient limitation of primary production in autotrophic habitats and food limitation of secondary production in heterotrophic habitats. Habitat fragmentation can therefore impose energetic constraints on the carrying capacity of aquatic ecosystems. The outcomes of ecosystem restoration through habitat creation will be determined by both functions provided by newly created aquatic habitats and the rates of hydraulic connectivity between them.

Keywords: habitat connectivity, fragmentation, primary production, secondary production, nutrient cycling, ecosystem restoration.

Ecologists historically have given little consideration to environmental spatial complexity and physical transport processes as mechanisms of population and community dynamics (Reiners and Driese 2001). A revolutionary perspective is emerging as researchers are now engaged in theoretical and empirical studies to reveal the ecological and evolutionary significance of ecosystems as open systems comprising interconnected and spatially heterogeneous subunits (Polis et al. 1997). Much of this research is aimed at discovering how the movement of species, life stages, individuals, and their genomes across heterogeneous landscapes shapes the evolution of communities and sustains populations. A major challenge is to unify the approaches and concepts of population and ecosystem ecology with those of landscape ecology (Polis et al. 2004; Lovett et al. 2005). This challenge is a frontier of ecological research because "most of the unresolved challenges in ecology arise from incomplete understanding of how biological and physical processes interact over multiple spatial and temporal scales" (Thompson et al. 2001, p. 23). The challenge represents an obstacle to effective management of ecosystems and their life-supporting functions. Many efforts to restore communities (Thompson et al. 2001) and sustain depleted stocks of individual species (Botsford et al. 1997) have failed for unknown reasons. Connectivity of functionally variable habitats may be a key to the design of actions for sustaining populations of harvested species (Roberts 1997) and biological diversity across increasingly fragmented landscapes (e.g., Köhler et al. 2003).

Biocomplexity is sustained not only by the dispersion of organisms and alleles but also by the transport of energy and resources (nutrients, food) across habitats and ecosystems (Pringle 2003; Lovett et al. 2005). Ecologists recognize the importance of resource subsidies from donor habitats to sustaining food webs in recipient habitats (Polis et al. 1997; Paetzold et al. 2005) and the export of organic matter from net autotrophic systems to support metabolism of net heterotrophic systems (Duarte and Cebrián 1996). However, the overall ecosystem significance of resource connectivity is largely unknown (but see Tockner et al. 2000; Holt 2004). Is resource connectivity a zero-sum process in which enhanced production in recipient systems is balanced by equal losses of production from

* E-mail: jecloern@usgs.gov.

Am. Nat. 2007. Vol. 169, pp. E000–E000.

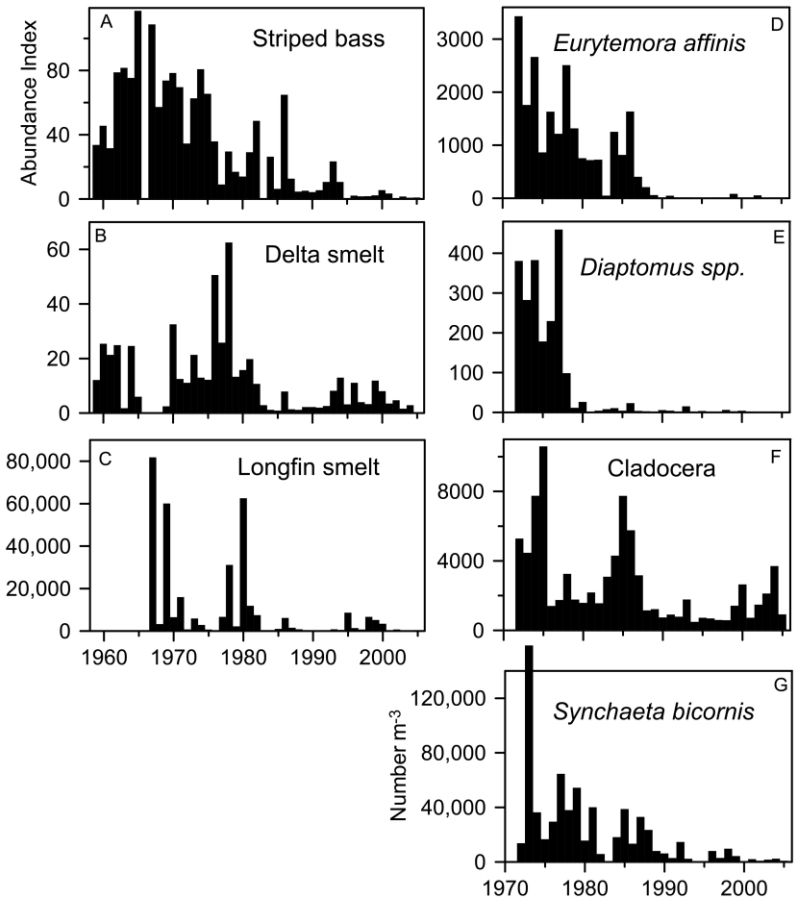

Figure 1: Population declines of pelagic fish (age-0 striped bass *Morone saxatilis*, delta smelt *Hypomesus transpacificus*, longfin smelt *Spirinchus thaleichthys*) from 1959 to 2005 and declines of zooplankton (copepods *Eurytemora affinis* and *Diaptomus* spp., cladocera, and rotifer *Synchaeta bicornis*) from 1972 to 2005 in the Sacramento–San Joaquin Delta. Fish abundance indices are computed from catch per unit effort during summer (or autumn for longfin smelt). Zooplankton indices are mean summer abundance. Data from the California Department of Fish and Game: http://www.delta.dfg.ca.gov.

donor systems? Or does overall system production respond in more complex ways to changes in connectivity through nonlinear processes of resource acquisition and utilization? Do emergent ecosystem properties, such as rates of primary and secondary production or nutrient cycling, vary with the strength of connectivity between functionally variable habitats? Resolution of these questions is a necessary step toward a unified spatial and temporal context (Thompson et al. 2001) for studying and understanding the full suite of ecosystem functions that sustain complex biological systems.

Habitat Connectivity and Pelagic Productivity: A Hypothesis from Monitoring Data

This study was motivated by a monitoring program that is documenting population collapses of pelagic organisms in the Sacramento–San Joaquin Delta, including multiple species of fish and zooplankton (fig. 1). Collectively, these data are compelling evidence that the carrying capacity of this ecosystem to sustain pelagic biota has been significantly degraded. Delta smelt (*Hypomesus transpacificus*) and longfin smelt (*Spirinchus thaleichthys*) are endemic to California's delta, and recent population estimates indicate that these species are at risk of extinction. The decadal-scale coherence between population collapses of fish and their zooplankton forage suggests that reduced production of supporting food webs is one mechanism of diminished carrying capacity. The magnitudes of aquatic habitat loss and fragmentation are well established: virtually all of the delta's original 1,400 km^2 of tidal marsh have been drained or diked (Nichols et al. 1986), and the tributary rivers have been dammed, channelized, and disconnected from their floodplains. The modeling analysis presented here

was designed to explore how disruption of connectivity between aquatic habitats might influence production in pelagic food webs supporting secondary consumers, such as planktivorous fish. The objective was to test a general null hypothesis: resource exchange (connectivity) between heterogeneous habitats is a zero-sum process such that subsidies to recipient habitats are balanced by losses from donor habitats, with no net effect on ecosystem-scale resource utilization.

Model Formulation and Hypothesis Testing

I used a model of nitrogen (N), phytoplankton (P), and zooplankton (Z) dynamics, as the simplest representation of a nutrient-producer-consumer system (e.g., Franks 2002), to test the null hypothesis for a pelagic ecosystem composed of two functionally variable habitats (denoted by subscripts 1, 2):

$$\begin{aligned}
\frac{dN_1}{dt} &= NS_1 + NR_1 - NU_1 - C \times (N_1 - N_2),\\
\frac{dP_1}{dt} &= PG_1 \times P_1 - PM \times P_1 - GR_1 - C \times (P_1 - P_2),\\
\frac{dZ_1}{dt} &= ZG_1 \times Z_1 - ZM_1 - C \times (Z_1 - Z_2),\\
\frac{dN_2}{dt} &= NS_2 + NR_2 - NU_2 + C \times (N_1 - N_2),\\
\frac{dP_2}{dt} &= PG_2 \times P_2 - PM \times P_2 - GR_2 + C \times (P_1 - P_2),\\
\frac{dZ_2}{dt} &= ZG_2 \times Z_2 - ZM_2 + C \times (Z_1 - Z_2).
\end{aligned} \tag{1}$$

Within each habitat, the nutrient resource N increases from external supply (NS) and internal regeneration (NR) and decreases through phytoplankton uptake (NU). Phytoplankton biomass grows at rate PG and is lost to mortality (PM) and zooplankton grazing (GR). Phytoplankton growth rate is prescribed as a temperature-dependent function of mean irradiance and a Michaelis-Menten function of nutrient concentration. Zooplankton biomass grows at rate ZG and is lost to density-dependent mortality (ZM). Zooplankton growth rate is temperature dependent and prescribed as a Michaelis-Menten function of phytoplankton biomass, with half-saturation constant K_P = 240 mg C m^{-3}. Process equations and parameters are presented in the appendixes.

The transport of N, P, and Z between habitats is computed as a turbulent diffusive process (e.g., De Angelis and Mulholland 2004). For example, mass transport MT (mg C day^{-1}) of phytoplankton biomass between habitats is

$$\mathrm{MT} = A \times D \times \left(\frac{P_1 - P_2}{L}\right), \tag{2}$$

where $(P_1 - P_2)$ is the biomass difference between habitats, A is area (m^2) of the interface between habitats, D (m^2 day^{-1}) is diffusivity, and L (m) is a characteristic length scale of turbulent diffusive transport. The rates of biomass change from transport between two habitats of equal volume V (m^3) are then

$$\begin{aligned}
\frac{dP_1}{dt} &= -\left(\frac{A \times D}{V \times L}\right) \times (P_1 - P_2),\\
\frac{dP_2}{dt} &= +\left(\frac{A \times D}{V \times L}\right) \times (P_1 - P_2).
\end{aligned} \tag{3}$$

The composite parameter $C = (A \times D)/(V \times L)$ is a connectivity rate having equivalent units (day^{-1}) to phytoplankton and zooplankton growth rates.

Phytoplankton growth rate is regulated by mean light exposure, which is inversely proportional to water column depth (Wofsy 1983). Simulations with the NPZ model (app. A) illustrate how shallow habitats sustain fast phytoplankton growth and net autotrophy (photosynthesis exceeds community respiration), whereas deep, light-limited habitats sustain low phytoplankton growth and net heterotrophy. Based on these results, I prescribed the model pelagic ecosystem as a shallow (H_1 = 5 m) autotrophic habitat connected to a deep (H_2 = 20 m) heterotrophic habitat and compared annual productivity and nutrient regeneration across a range of connectivity rates between C = 0 and 10 day^{-1}.

Each simulation computed daily N, P, and Z in both habitats, using initial conditions: $N_1 = N_2$ = 500 mg N m^{-3}; $P_1 = P_2$ = 35 mg C m^{-3}; $Z_1 = Z_2$ = 3.5 mg C m^{-3}. Simulations prescribed annual cycles of water temperature and solar irradiance to represent a dynamic system forced by daily changes in inputs of heat and light energy. System dynamics were indexed as changes in the overall mean nutrient concentration N_S (=average of annual mean N_1 and N_2), phytoplankton biomass P_S, and zooplankton biomass Z_S in the two equal-volume habitats. Daily primary productivity (= PG × P) was summed over the year to compute annual gross primary production GPP (g C m^{-3} year^{-1}) for each habitat, and these were averaged to yield system primary production GPP_S. System rates of nutrient regeneration NR_S (g N m^{-3} year^{-1}) and zooplankton secondary production ZP_S (g C m^{-3} year^{-1}) were similarly computed as the average of annual rates in the two habitats. These overall mean values across habitats were used to test the hypothesis that rates of ecosystem production

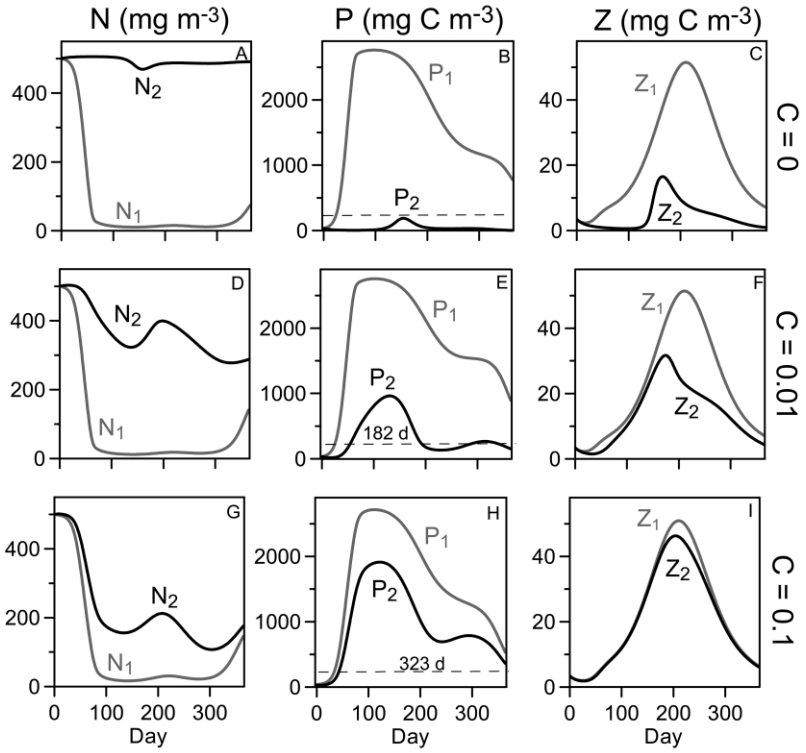

Figure 2: Annual simulations of nutrient concentration N, phytoplankton biomass P, and zooplankton biomass Z, comparing simulations using three connectivity rates *C* between a shallow (*gray lines*) and a deep (*black lines*) habitat. The dashed line (P = 240) indicates the food concentration supporting half-maximal zooplankton ingestion and growth.

and nutrient cycling do not vary with changes in habitat connectivity.

An initial set of simulations depicted a two-habitat pelagic ecosystem in which *C* is fixed and nutrient supply rate is zero. An additional set of simulations varied the connectivity rate *C* in proportion to daily fluctuations in physical forcings that drive hydraulic connectivity: tides, wind, river discharge, and seasonal peak flows that inundate floodplains. Factors for tide-, wind-, and river-driven connectivity were daily measures, normalized to annual means for 2000, of tidal amplitude (NOAA, http://tidesandcurrents.noaa.gov) and wind stress (California Irrigation Management Information System, http://www.cimis.water.ca.gov/cimis/data.jsp) in the Sacramento–San Joaquin Delta and Sacramento River discharge (California Department of Water Resources, http://www.iep.water.ca.gov/dayflow/index.html). Floodplain inundation was prescribed for January–April, characteristic of managed floodplains on the Sacramento River (Sommer et al. 2001). A final simulation depicted variable nutrient influx to the deep habitat, computed as normalized river discharge multiplied by a mean influx of 0.5 mg N m^{-3} day^{-1}.

Results

Seasonal NPZ Dynamics

Simulated seasonal dynamics of nutrient concentration and plankton biomass varied with habitat connectivity rate, primarily in the deep habitat. A baseline simulation of zero connectivity compared annual NPZ cycles in the two habitats as isolated, closed systems (fig. 2*A*–2*C*). Phytoplankton biomass in the shallow habitat (P_1) grew rapidly during spring, depleted the initial high nutrient stock (N_1), and then declined slowly but remained high enough ($P_1 > K_P$) to sustain food-saturated zooplankton growth and high zooplankton biomass (Z_1). Light limitation was so severe in the deep habitat that phytoplankton biomass (P_2) remained low and always less than K_P, indicating chronic food limitation of zooplankton growth. Annual mean zooplankton biomass in the deep habitat (Z_2) was only 4.5 mg C m^{-3} compared with 23 mg C m^{-3} in the shallow habitat. This baseline simulation illustrates the functional variability of pelagic systems. Light energy is sufficient in shallow habitats to drive efficient conversion of nutrient resources into biomass, creating a nutrient-limited state in which production is sustained by nutrient

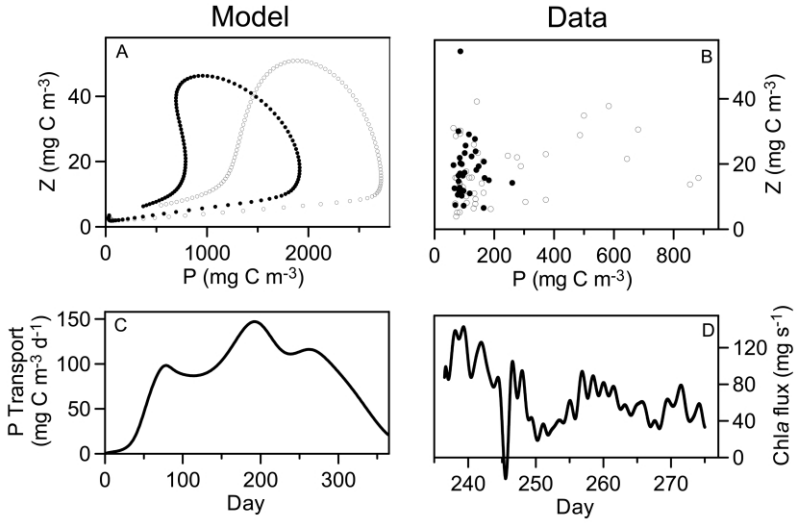

Figure 3: Comparisons between simulations with a two-habitat NPZ model ($C = 0.1$; see fig. 2*G*–2*I*) and data collected in a shallow (*open circles*) and a deep (*filled circles*) habitat of the Sacramento-San Joaquin Delta. *A*, *B*, absence of correlation between zooplankton biomass Z and phytoplankton biomass P; *C*, simulated daily transport of phytoplankton biomass from the shallow to the deep habitat; *D*, tidally averaged dispersive chlorophyll *a* flux from a shallow lake to a deep channel, measured with an acoustic Doppler current meter and fluorometers (redrawn from Lopez et al. 2006).

regeneration. Low mean irradiance of deep habitats limits phytoplankton growth and nutrient uptake, leaving the nutrient resource unutilized.

Seasonal dynamics in the deep habitat changed when the habitats were connected, even at a slow rate (fig. 2*D*–2*F*). At $C = 0.01$ day^{-1}, mean annual phytoplankton biomass P_2 increased nearly tenfold, from 40 to 360 mg C m^{-3}. This biomass increase was a consequence of transport from the shallow habitat, and this exogenous supplement to the food resource sustained higher zooplankton growth rates and biomass in the deep habitat, where P_2 exceeded K_P during 182 days of the simulation (fig. 2*E*). Amplified zooplankton production in the deep habitat was not balanced by a corresponding decline of zooplankton production in the shallow habitat because phytoplankton biomass P_1 remained high enough there to sustain near-optimal zooplankton growth (fig. 2*E*). Connectivity of the nutrient pools between habitats was also important as the deep habitat became a nutrient source to sustain high primary productivity in the shallow habitat. This is reflected in the increased depletion of nutrients (N_2) in the deep habitat (fig. 2*D*).

At $C = 0.1$ day^{-1}, phytoplankton biomass increased even further in the deep habitat because a larger fraction of primary production was exported from the shallow habitat (fig. 2*G*–*2I*). Phytoplankton biomass remained high enough to sustain near-optimal zooplankton growth in both habitats, and zooplankton biomass and production in the deep habitat were nearly identical to those in the shallow habitat. At this fixed connectivity rate, the import of phytoplankton biomass exceeded primary production and contributed 54% of the total annual phytoplankton supply to sustain zooplankton secondary production in the deep habitat. The deep habitat became a more important nutrient source to support primary production in the shallow habitat. At $C = 0.1$ day^{-1}, computed N import sustained 24% of annual phytoplankton uptake in the shallow habitat.

Simulations with this two-habitat NPZ model are consistent with some key patterns and processes measured in a shallow lake connected by tidal mixing to a deep-channel system within the Sacramento–San Joaquin Delta. Both model and measurements show zero correlation between zooplankton and phytoplankton biomass, either within or between habitats, even though zooplankton growth is food limited in the deep habitats (fig. 3*A*, 3*B*). Estimated rates of zooplankton ingestion exceeded rates of primary production in the deep-channel system, implying an exogenous source of food (Lopez et al. 2006). Continuous measurements of tidal currents and chlorophyll fluorescence revealed a net dispersive transport of phytoplankton biomass from the shallow lake to the deep channel (fig. 3*D*), verifying that the shallow habitat is a source of phytoplankton biomass to fuel secondary production in the adjacent channel. This process of steady phytoplankton transport from the shallow to the deep habitat is simulated by the NPZ model (fig. 3*C*).

Habitat Connectivity and Ecosystem Productivity

As connectivity increases, the convergence of NPZ dynamics between habitats suggests that there may be limits to the amplification of system production by resource exchange. Simulations over a range of C showed that the net outcome of habitat connectivity was increased efficiency in the conversion of nutrients into consumer biomass, revealed as declining system N_S and increasing system P_S and Z_S as connectivity increased (fig. 4*A*–4*C*). As C increased from 0 to 0.1 day^{-1}, system mean zooplankton biomass increased from 13.7 to 21.7 mg C m^{-3} because gains in Z_2 supported by phytoplankton import exceeded losses of Z_1 from phytoplankton export (fig. 4*C*).

Mean system primary production GPP_S increased from 42 to 63 g C m^{-3} year^{-1} (fig. 4*E*) as connectivity rate was increased from 0 to 0.1 day^{-1}; enhancement of system production resulted from both phytoplankton transport to the nutrient-rich deep habitat (fig. 2*A*) and nutrient transport to the shallow habitat. Mean system nutrient regeneration rate NR_S increased from 7.2 to 10.8 g N m^{-3} year^{-1} (fig. 4*D*), and regeneration enhancement occurred in the deep habitat, where the import and consumption of phytoplankton biomass accelerated with increasing connectivity. Import of phytoplankton biomass amplified zooplankton production even more in the deep habitat (fig. 4*F*), leading to a 73% increase in system zooplankton production ZP_S, from 3.0 ($C = 0$) to 5.2 ($C = 0.1$) g C m^{-3} year^{-1}.

In this two-habitat NPZ system, overall consumer biomass and secondary production varied with habitat connectivity through its influence on the distribution of primary producer biomass and regenerated nutrients. Transport of both quantities was necessary to sustain high secondary production. When the transports of N and P were set individually to zero, overall zooplankton production was low (fig. 4*F*, *diamond*) because zooplankton in the deep habitat became isolated from the exogenous food supply or because primary producers in the shallow habitat became isolated from the exogenous nutrient supply.

In these simulations, maximum rates of system nutrient regeneration and biomass production occurred when the connectivity rate was of the same magnitude (~0.1 day^{-1}) as the growth rate of phytoplankton in the shallow (donor) habitat. Robustness of this result was explored with simulations depicting habitats where resource exchange is driven by daily fluctuations in tidal currents, wind stress, or river flow (fig. 5*C*–5*G*). System primary and zooplankton secondary production (fig. 5*A*, 5*B*) varied as asymptotic functions of C/PG_1, the annual mean ratio of con-

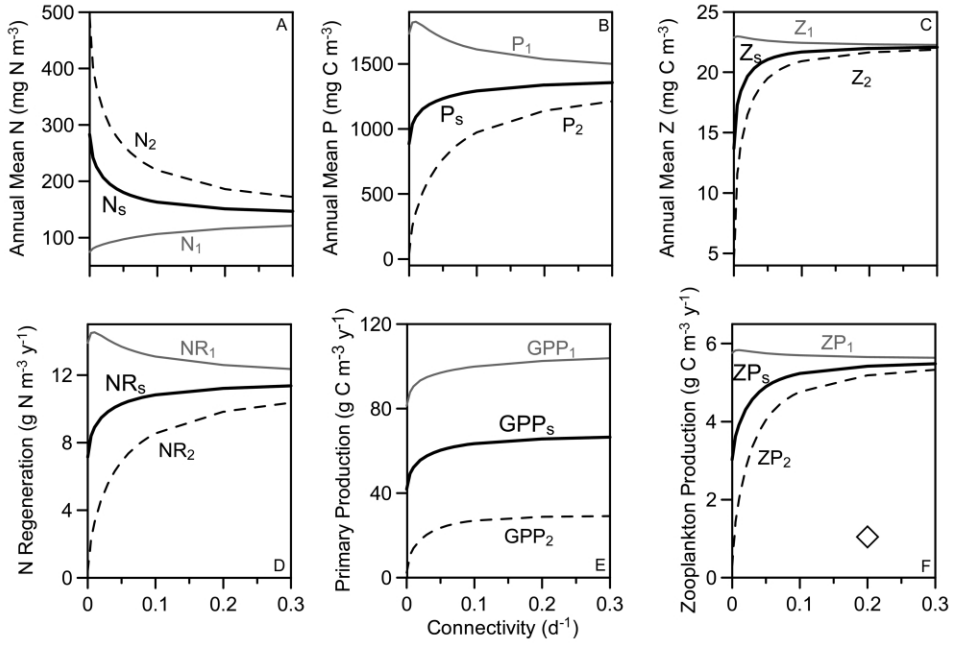

Figure 4: Emergent properties of a simulated pelagic system versus connectivity rate C between a shallow autotrophic (*gray lines*) and deep heterotrophic (*dashed lines*) habitat. *A*–*C*, Annual mean nutrient concentration and phytoplankton and zooplankton biomass (N_1 = shallow habitat; N_2 = deep habitat; N_S = mean of N_1, N_2); *D*–*F*, annual rates of nutrient regeneration and primary and zooplankton secondary production (NR_S = mean of NR_1, NR_2, etc.). Diamond (*F*) shows simulation results when phytoplankton transport or nutrient transport were set to zero.

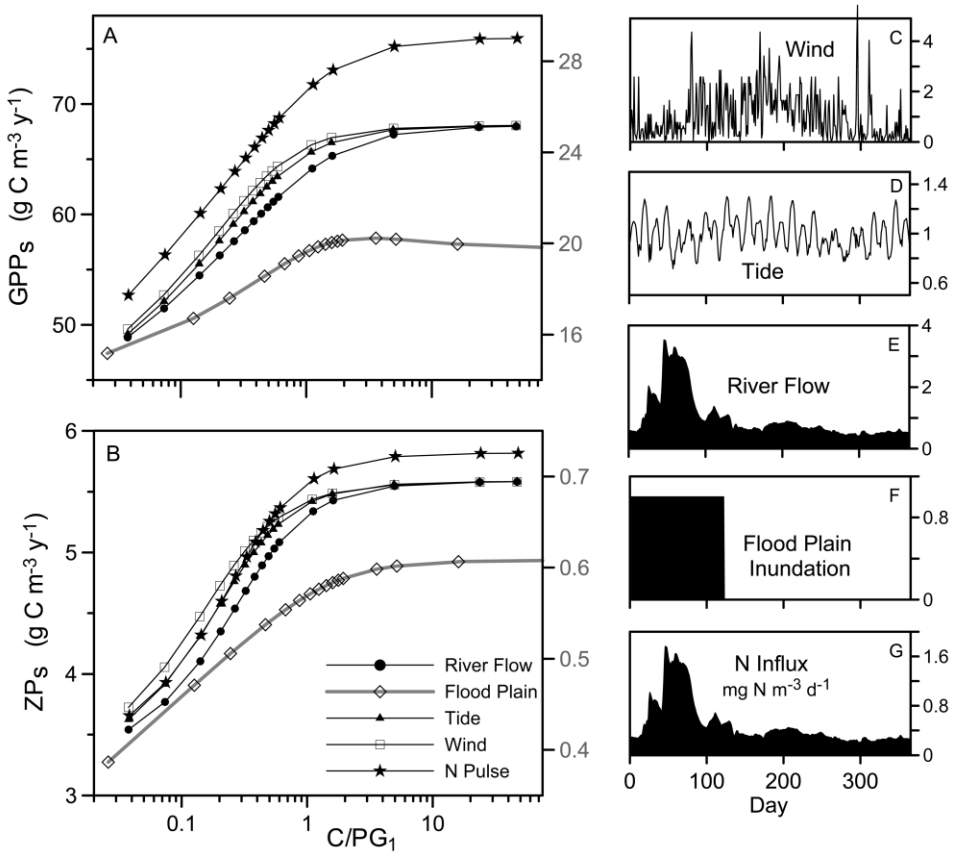

Figure 5: System gross primary production GPP_S (*A*) and zooplankton secondary production ZP_S (*B*) versus the nondimensional parameter C/PG_1 for five simulation experiments; floodplain simulations are plotted using right-hand *Y*-axes. Connectivity *C* was varied in proportion to normalized daily fluctuations in wind stress (*C*), tidal amplitude (*D*), river flow (*E*), or floodplain inundation (*F*); or N influx was varied with river flow (*G*).

nectivity rate to phytoplankton growth rate in the shallow habitat. Daily fluctuations in *C* had little effect on system production, but rates of primary and secondary production were highest with prescription of a continuing nutrient influx and greatly reduced when the habitats were disconnected by low river flow, depicting the seasonal draining of a floodplain. Optimal system production varied with nutrient supply rate and intermittency of habitat connectivity, but primary and secondary production were uniformly suboptimal when $C/PG_1 < 1$ and approached optima as the ratio C/PG_1 approached 1.

Discussion

Habitat Connectivity and Ecosystem Productivity

Simulations with a two-habitat NPZ model show that resource exchange across aquatic habitats is not necessarily a zero-sum process, and they reveal mechanisms through which habitat connectivity can amplify rates of nutrient regeneration and primary and secondary production (fig. 4*D*–4*F*). This result is a consequence of ecosystem attributes prescribed in the model: connectedness of habitats that provide different functions and dispersive (gradient-driven) transport between these habitats. Simulation results would be different where resource exchange is driven by advection (e.g., Roughgarden et al. 1988) or animal migrations (e.g., Jager et al. 2001). Results also might differ when other processes of nutrition are included, such as algal mixotrophy or zooplankton omnivory, although mixotrophy becomes most important in oligotrophic waters (Troost et al. 2005) and zooplankton growth is tightly coupled to the phytoplankton food supply, even in river-estuarine systems receiving large detrital inputs (Sobczak et al. 2002; Müller-Solger et al. 2002).

Simulations presented here were motivated by a field experiment in which NPZ dynamics were compared in a shallow tidal lake and a deep channel connected by tidal mixing (Lopez et al. 2006). However, the model was

conceived as a general depiction of functionally variable habitats linked by hydraulic connectivity, such as river-floodplain systems (Tockner et al. 2000), intertidal and deep subtidal estuarine habitats (Caffrey et al. 1998), free-flowing stream waters and underlying transient storage zones (DeAngelis and Mulholland 2004) or lateral recirculation zones (Reynolds 2000), littoral wetlands and pelagic lake habitats (Larmola et al. 2004), or streams and riparian forests (Power et al. 2004). In each case, a spatial domain of high primary productivity exports organic matter as algal biomass or detritus to support secondary production in a low-productivity spatial domain, and/or a heterotrophic domain exports regenerated nutrients to support primary production in an autotrophic domain.

Across a range of scenarios representing this diversity of connected habitat types, simulations revealed a consistent functional relationship between ecosystem-scale productivity and habitat-scale connectivity (fig. 5*A*, 5*B*). Therefore, primary and secondary productivity in spatially complex pelagic systems can be limited by resource exchange when connectivity rate is slow, and they can attain optima when connectivity is fast. The critical connectivity rate is defined by the characteristic population growth rate of producers in donor habitats. The upper limit to system productivity is imposed by factors such as exogenous nutrient supply (e.g., riverine nutrient input; fig. 5*G*) and intermittency of habitat connectivity (e.g., seasonal inundation of floodplains; fig. 5*F*), but the realization of that potential productivity is set by the mean rates of resource exchange. System productivity appears to be insensitive to daily-scale variability of connectivity from processes such as wind-driven mixing between pelagic and littoral habitats (fig. 5*C*), tidal dispersion between deep and shallow estuarine habitats (fig. 5*D*), or flow-driven exchange across river habitats (fig. 5*E*).

A key to the productivity-connectivity relationship is the model representation of zooplankton ingestion and growth as an asymptotic function of food availability (eq. [B11]). This functional form, observed in laboratory measurements of rotifer, cladoceran, and copepod feeding rates (Hansen et al. 1997), reflects a mechanical and metabolic constraint on the capacity of these consumers to capture and assimilate food particles. Food ingestion by crustacean zooplankton becomes saturated at phytoplankton biomass of ~300–500 mg C m^{-3}. Simulations here revealed maximum systemwide secondary production when primary production in the donor habitat maintained phytoplankton biomass above this saturating food level in both habitats. In the absence of connectivity, the donor habitat produced phytoplankton biomass beyond that which could be assimilated to fuel zooplankton secondary production. When some of that biomass was exported to a food-limited habitat, the subsidy fueled further zooplankton production in the recipient habitat. The export of phytoplankton biomass from the donor system did not diminish local secondary production because zooplankton food ingestion was already saturated by high phytoplankton biomass. Coherent model results and measurements (fig. 3) reveal how pelagic carbon flow and secondary production are influenced by the interactions between large-scale constraints on habitat connectivity and small-scale constraints on the capacity of individual organisms to capture food particles—an ecological outcome of biological and physical processes operating over different spatial scales (Thompson et al. 2001).

Scaling Rules of Pelagic Ecosystem Productivity

Phytoplankton photosynthesis and growth are highly constrained by mean photon flux density because light is rapidly attenuated by water and suspensoids (e.g., Diehl 2002). Mean irradiance in a mixing water column is inversely proportional to optical depth, the product of habitat depth H and turbidity (light attenuation coefficient k). Shallow/transparent waters ($Hk < 10$) provide sufficient light energy to sustain system autotrophy through fast phytoplankton growth and conversion of dissolved nutrients into plankton biomass (fig. 6; Wofsy 1983). Deep/turbid waters ($Hk > 20$) sustain high nutrient concentrations characteristic of net heterotrophic habitats because photosynthesis and nutrient uptake are limited by low mean irradiance. The nondimensional parameter Hk is a simple and powerful measure of pelagic habitat function along the continuum from strong autotrophy to strong heterotrophy.

Simulations presented here suggest a second scaling rule to define the constraint on productivity by resource exchange across habitats. System plankton biomass and productivity are optimized when the characteristic rates of resource transport C and biological production PG_1 are approximately equal, such that spatial gradients of nutrients and biomass are dissipated (fig. 4). When transport is slow relative to biological processes ($C/PG_1 < 1$), biomass accumulates and nutrients become depleted and limit production in autotrophic habitats while nutrients accumulate unutilized in heterotrophic habitats. As transport increases relative to growth, resource exchanges accelerate the conversion of nutrients into biomass. Overall system production can therefore be constrained by the balance between rates of transport, production of organic carbon and regeneration of dissolved nutrients. For this simple two-habitat pelagic ecosystem, primary and secondary production are limited by resource transport when $C/PG_1 < 1$, and this rule is robust across variations in connectivity rate and nutrient influx (fig. 5*A*, 5*B*). This model-derived rule is consistent with observations of optimized

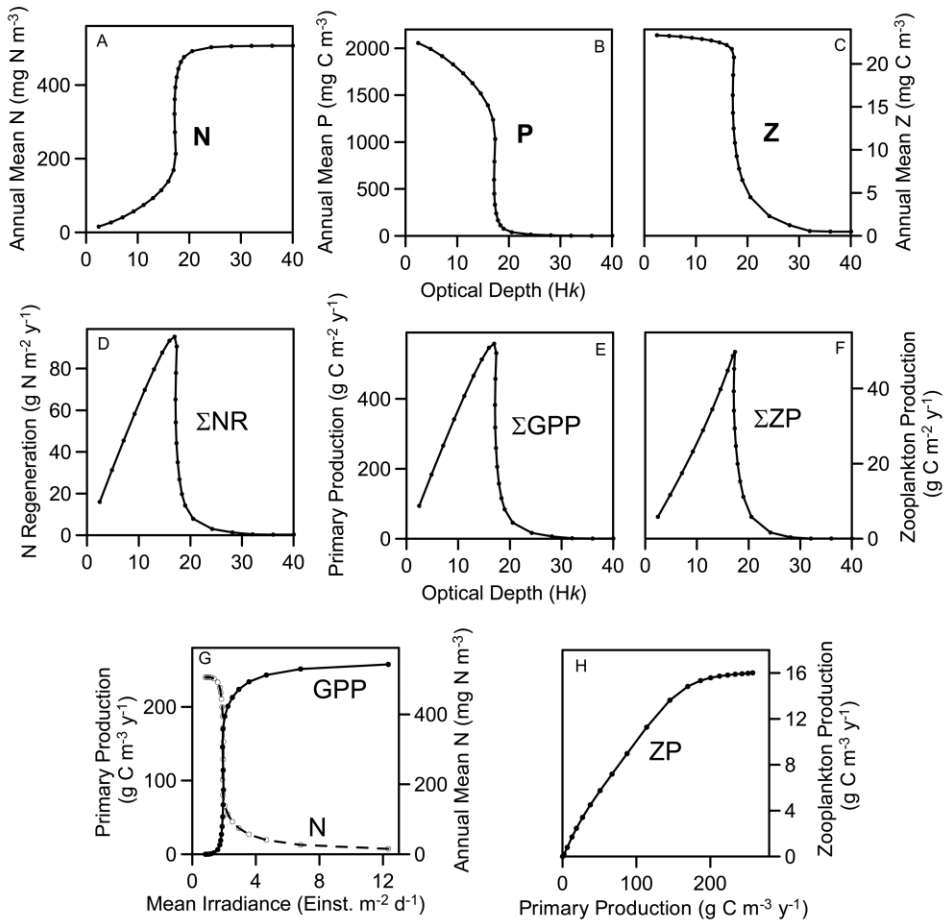

Figure 6: Emergent properties of a simulated NPZ system as influenced by habitat optical depth *Hk*. *A–C*, annual mean nutrient concentration and phytoplankton and zooplankton biomass; *D–F*, annual depth-integrated rates of nutrient regeneration ΣNR, gross primary production ΣGPP, and zooplankton secondary production ΣZP. *G*, Strong regulation of primary production (*solid line*) by light limitation until nutrients (*dashed line*) become depleted. *H*, Tight coupling between zooplankton and phytoplankton production within a closed habitat.

primary production in river-floodplain systems based on the balance between algal growth and transport rates (Tockner et al. 2000).

The technology now exists for measuring resource fluxes with acoustic Doppler current profilers and sensors for chlorophyll (fig. 3*D*), organic carbon, dissolved nutrients, and plankton abundance/size distribution. Coupled with traditional measures of standing stocks and production/regeneration rates, resource flux measurements between habitats provide the information required to develop mechanistic understanding of how habitat-scale functional variability propagates to drive ecosystem-scale variability of primary and secondary production and to test empirically the model-derived rule of suboptimal productivity when $C/\mathrm{PG} < 1$.

Implications for the Carrying Capacity of Damaged Ecosystems

The ecological significance of spatial connectivity has largely been explored as a process that sustains species diversity, food web complexity, and community stability, partly as a framework for understanding the consequences of habitat fragmentation. Model results presented here identify processes through which hydraulic connectivity can also impose energetic and resource constraints on the carrying capacity of pelagic systems. The nearly twofold variability in simulated zooplankton production across gradients of connectivity strength (fig. 4*F*) represents a comparable variability in the potential carbon supply to secondary consumers such as planktivorous fish. Ecosystem carrying capacity can therefore be determined by both

the functional variability across habitat mosaics and the transport of primary-producer biomass to consumers and regenerated nutrients to primary producers.

The two scaling rules above provide a quantitative context for understanding how landscape transformations can reduce the productivity and carrying capacity of aquatic ecosystems. Conversion of wetlands into agricultural land and dredging of channels in the Sacramento–San Joaquin Delta have reduced the area of shallow (low *Hk*) autotrophic habitats and increased the volume of deep (high *Hk*) heterotrophic habitats. The transformed waterscape has high nutrient concentrations but sustains low primary production of only 75 g C m^{-2} $year^{-1}$ (Jassby et al. 2002)—comparable to primary production in oligotrophic regions of the open ocean. Habitat fragmentation contributes to this low system production because dikes, barriers, and flow diversions block or damp hydraulic connectivity within the delta ecosystem.

Species at multiple trophic levels are at risk of extinction (fig. 1), and the diminished carrying capacity of this ecosystem is the consequence of multiple stressors, including habitat loss and fragmentation, water diversions that export 30% of autochthonous primary production (Jassby et al. 2002), and alien species that exacerbate the food limitation of zooplankton growth (Lopez et al. 2006). Strategies to rehabilitate carrying capacity and sustain species on the brink of extinction require actions to minimize each stressor, and strategic plans are evolving to restore ecological functions, including primary production, through habitat creation. As shown here, the outcomes of habitat creation will depend on the rates and pathways of nutrient and food resource connectivity across future habitat mosaics. Direct measurement of resource connectivity is one key to understanding ecosystem dynamics and optimizing the outcomes of habitat rehabilitation. The scaling rule developed here suggests that carrying capacity is optimized when the rates of transport match the rates of primary production. Ecosystem restoration through adaptive management provides experimental opportunities to test the validity of this design principle.

Acknowledgments

This study was supported by the U.S. Geological Survey Programs of Hydrologic Research and Toxic Substances Hydrology, and by the CALFED Bay-Delta Program's Ecosystem Restoration Program. R. Baxter (California Department of Fish and Game) provided data in figure 1. L. Lucas and T. Schraga provided data in figure 3*D*, and L. Lucas provided helpful guidance in an early version of this article. Two anonymous reviewers provided careful evaluations and thoughtful guidance that markedly improved the quality and clarity of this article.

APPENDIX A

The NPZ Model

The NPZ model comprises three ordinary differential equations that define coupled dynamics of a limiting nutrient N (mg N m^{-3}), phytoplankton biomass P (mg C m^{-3}), and zooplankton biomass Z (mg C m^{-3}) in a homogeneous water column of depth H (m):

$$\frac{d\mathrm{P}}{dt} = \mathrm{PG} \times \mathrm{P} - \mathrm{PM} \times \mathrm{P} - \mathrm{GR},$$

$$\frac{d\mathrm{N}}{dt} = \mathrm{NS} - \mathrm{NU} + \mathrm{NR}, \tag{A1}$$

$$\frac{dZ}{dt} = \mathrm{ZG} \times \mathrm{Z} - \mathrm{ZM}.$$

Phytoplankton biomass grows at light- and nutrient-regulated rate PG (day^{-1}) and is lost to mortality (PM) and zooplankton grazing (GR). Nutrient concentration N is determined by exogenous supply rate NS (mg N m^{-3} day^{-1}), uptake by phytoplankton (NU), and regeneration (NR) from mortality and metabolism of phytoplankton and consumers. Zooplankton biomass is determined by the balance between food- and temperature-dependent growth rate ZG (day^{-1}) and density-dependent mortality (ZM). Daily gross primary productivity GPP (mg C m^{-3} day^{-1}) is PG × P, and zooplankton secondary productivity ZP (mg C m^{-3} day^{-1}) is ZG × Z. Annual rates of depth-integrated nutrient regeneration (ΣNR, g N m^{-2} $year^{-1}$), gross primary production (ΣGPP, g C m^{-2} $year^{-1}$), and zooplankton production (ΣZP, g C m^{-2} $year^{-1}$) are computed as the sum of daily rates multiplied by depth H. Parameters and formulations for each process are detailed in appendix B.

The coupled equations were solved over annual periods, using the application STELLA (http://www.iseesystems.com) with a computational time step of 0.02 days and fourth-order Runge-Kutta integration (other computational procedures did not always conserve C or N mass). Water temperature T (5°–25°C) and photosynthetically active incident irradiance E (10–50 einsteins m^{-2} day^{-1}) were prescribed as periodic functions of time (t) to describe a dynamic system forced by daily changes in inputs of heat and light energy:

$$T = 15 - 10 \times \cos\left(2\pi \frac{t - 31}{365}\right), \tag{A2}$$

$$E = 10 + 40 \times \sin\left(\pi \times \frac{t}{365}\right)^{1.3}. \tag{A3}$$

Initial values were fixed at N = 500 mg N m^{-3}, P = 35 mg C m^{-3}, and Z = 3.5 mg C m^{-3}. For simulation results shown below, NS was fixed at zero to depict a habitat where exogenous nutrient inputs are balanced by exports.

Habitat Functions versus Habitat Depth

Simulations with this NPZ model are consistent with the principles that (1) phytoplankton growth rate scales inversely with habitat depth because of the vertical attenuation of light (e.g., Wofsy 1983; Diehl 2002) and (2) rates of secondary production and nutrient cycling scale with primary production. For a baseline light attenuation coefficient k of 1 m^{-1} and water depth $H = 5$ m, NPZ simulations describe an annual cycle of rapid phytoplankton growth and nutrient uptake during spring followed by nutrient depletion and declining phytoplankton biomass, with zooplankton biomass growing through summer and peaking at 52 mg C m^{-3} (fig. 2*A*–2*C*). Simulations for a deeper ($H = 20$ m) habitat showed the damping effects of light limitation: water column mean irradiance was insufficient to sustain phytoplankton growth except during a brief period in midsummer, so the nutrient stock remained unutilized. Low phytoplankton biomass imposed chronic food limitation of zooplankton growth, and the peak zooplankton biomass was only 16.5 mg C m^{-3} in the light-limited deep habitat (fig. 2*A*–2*C*). The shallow habitat functioned as a net autotrophic system (net producer of phytoplankton biomass), whereas the deep habitat was net heterotrophic.

Mean light exposure of phytoplankton cells in a mixed water column is determined by water depth H and turbidity k, and phytoplankton growth rate is inversely proportional to the optical depth Hk (Wofsy 1983). Annual simulations of NPZ dynamics across a range of H from 1 to 40 m reveal the patterns of functional variability among pelagic habitats as optical depth and light limitation progressively increase (fig. 6). Mean annual nutrient concentration was near zero at $H = 1$ m (optical depth = 2), and mean N progressively increased as optical depth approached 20 (fig. 6*A*). The magnitude of nutrient depletion in a closed system is a measure of net phytoplankton uptake, so this pattern reflects large variability across habitat depths in the rates of nutrient assimilation and primary production. The simulations reveal a strong inverse relationship between mean annual phytoplankton biomass and optical depth (fig. 6*B*), consistent with other pelagic models (Wofsy 1983). This variability in the food supply to consumers generates variability across habitats in their capacity to sustain zooplankton biomass (fig. 6*C*).

Depth-integrated rates of nutrient regeneration, primary production, and zooplankton production were maximum at optical depth $Hk = 17$ (fig. 6*D*–6*F*); these areal rates were nutrient and depth limited in shallow habitats and light limited in deep habitats. Therefore, depth-integrated rates of pelagic nutrient cycling, primary production, food supply to consumers, and system metabolism all vary as unimodal functions of habitat depth. The resource regulation of these functions is revealed in figure 6*G*, showing a sharp increase in primary production with mean irradiance until the nutrient resource becomes limiting. The propagation of this resource regulation to the next trophic level is revealed by the strong correlation between simulated zooplankton secondary production and primary production in a closed system (fig. 6*H*).

APPENDIX B

Model Parameters and Process Rates

Phytoplankton growth rate PG (day^{-1}) is computed from temperature-dependent maximum growth rate PG_{max} and fractional reductions from nutrient (N) and light (I) limitation (Murray and Parslow 1997):

$$PG = PG_{max} \times f(N) \times f(I), \tag{B1}$$

$$PG_{max} = 1.25 \times 2^{(T-15)/10}, \tag{B2}$$

$$f(N) = \frac{N}{N + K_N}, \tag{B3}$$

$$f(I) = \min\left[\frac{I}{I_{max}}, 1\right]. \tag{B4}$$

The temperature (T) dependence of PG_{max} is based on growth rate measurements compiled by Tett et al. (1986). Nutrient limitation is described as a Michaelis-Menten function with the half-saturation constant $K_N = 14$ mg N m^{-3} (Chen et al. 1997). The light resource is computed as mean water column irradiance I (einsteins m^{-2} day^{-1}, photosynthetically active radiation):

$$I = \frac{E}{Hk}(1 - e^{-Hk}), \tag{B5}$$

where E is daily surface irradiance (eq. [A3]) and k is the light attenuation coefficient (m^{-1}):

$$k = k_b + k_p. \tag{B6}$$

Quantity k_b is nonalgal turbidity (fixed at $k_b = 1$ m^{-1}, characteristic of the Sacramento–San Joaquin Delta); k_p is the phytoplankton component of turbidity ($= 0.025 \times$ P/CChl*a*, where CChl*a* = carbon : chlorophyll *a* ratio), us-

ing the chlorophyll *a*-specific attenuation coefficient of 0.025 m^2 mg^{-1} Chl*a* (Tett 1990) and assuming the phytoplankton CChl*a* = 35 (Cloern et al. 1995). The irradiance sustaining optimal growth is computed as

$$I_{max} = 15.3 \times 2^{(T-15)/10}, \quad \text{(B7)}$$

where the constant 15.3 was computed from an empirical model relating phytoplankton photosynthetic assimilation rate (PB) and growth rate (Cloern et al. 1995):

$$PG = 0.85 \times \frac{PB}{CChla} - 0.015. \quad \text{(B8)}$$

The assimilation rate PB (mg C mg^{-1} Chl*a* day^{-1}) was computed from the linear relation between depth-integrated photosynthesis and irradiance determined with ^{14}C-uptake assays in the nutrient-rich Sacramento–San Joaquin River Delta (Jassby et al. 2002):

$$PB = 3.36 \times I. \quad \text{(B9)}$$

Then,

$$PG = 0.85 \times 3.36 \times \frac{I}{CChla} - 0.015. \quad \text{(B10)}$$

This equation was set equal to the maximum phytoplankton growth rate of 1.25 day^{-1} (eq. [B2]) and solved for I_{max} at the reference temperature of $T = 15°C$. Phytoplankton mortality PM is fixed at a constant biomass-specific rate of 0.1 day^{-1} (Ross et al. 1993).

Zooplankton biomass is computed as the balance between daily growth and predation, assuming one generic zooplankton stock dependent solely on the phytoplankton food resource. The approach uses equations developed by Hansen et al. (1997) from a comprehensive synthesis of laboratory feeding measurements of freshwater and marine protozoa, rotifers, copepods, and cladocera. The zooplankton biomass-specific ingestion rate ZI (day^{-1}) is computed as a temperature-dependent function of phytoplankton biomass:

$$ZI = ZI_{max} \times \frac{P}{P + K_P}, \quad \text{(B11)}$$

$$ZI_{max} = 2.1 \times 2.8^{(T-20)/10}, \quad \text{(B12)}$$

$$K_P = 240 \text{ mg C } m^{-3}. \quad \text{(B13)}$$

Zooplankton grazing rate GR (mg C m^{-3} day^{-1}) is ZI × Z, and zooplankton growth rate ZG (day^{-1}) = 0.33 × ZI, where the growth yield of 0.33 is the mean of laboratory measurements for 33 zooplankton species (Hansen et al. 1997). The unassimilated fraction of zooplankton ingestion (= 0.67 × ZI) represents metabolic and waste losses that do not contribute to biomass growth.

Zooplankton mortality is the critical closure term of NPZ models (Franks 2002), and the approach here is based on assumptions that all mortality is from predation, providing an estimate of potential forage supply to planktivorous fish, and that predation is density dependent (Steele and Henderson 1992): $ZM = 0.02 \times Z^2$. This equation constrains zooplankton biomass to an upper limit of ~50 mg C m^{-3}, the maximum zooplankton biomass commonly observed in high-nutrient freshwater and estuarine ecosystems (e.g., Lopez et al. 2006).

Nutrient concentration N is determined by the balance between a prescribed supply rate NS (mg N m^{-3} day^{-1}), phytoplankton uptake rate NU, and regeneration rate NR:

$$NU = 0.176 \times GPP, \quad \text{(B14)}$$

$$NR = 0.176 \times (PM \times P + 0.67 \times GR + 0.71 \times ZM). \quad \text{(B15)}$$

Nutrient mass is conserved if uptake and regeneration are computed from carbon fluxes using a fixed C : N ratio, here the Redfield ratio of 0.176 mg N mg^{-1} C. Regeneration is from phytoplankton mortality (PM × P) and metabolism and waste production of zooplankton (0.67 × GR) and zooplankton predators (0.71 × ZM), assuming a 29% growth efficiency of carnivorous fish (Hanson et al. 1997).

Literature Cited

Botsford, L. W., J. C. Castilla, and C. H. Peterson. 1997. The management of fisheries and marine ecosystems. Science 277:509–515.

Caffrey, J. M., J. E. Cloern, and C. Grenz. 1998. Changes in production and respiration during a spring phytoplankton bloom in San Francisco Bay, California, USA: implications for net ecosystem metabolism. Marine Ecology Progress Series 172:1–12.

Chen, C., D. A. Wiesenburg, and L. Xie. 1997. Influences of river discharge on biological production in the inner shelf: a coupled biological and physical model of the Louisiana-Texas Shelf. Journal of Marine Research 55:293–320.

Cloern, J. E., C. Grenz, and L. Videgar-Lucas. 1995. An empirical model of the phytoplankton carbon : chlorophyll ratio—the conversion factor between productivity and growth rate. Limnology and Oceanography 40:1313–1321.

DeAngelis, D. L., and P. J. Mulholland. 2004. Dynamic consequences of allochthonous nutrient input to freshwater systems. Pages 12–24 *in* G. A. Polis, M. E. Power, and G. R. Huxel, eds. Food webs at the landscape level. University of Chicago Press, Chicago.

Diehl, S. 2002. Phytoplankton, light, and nutrients in a gradient of mixing depths: theory. Ecology 83:386–398.

Duarte, C. M., and J. Cebrián. 1996. The fate of marine autotrophic production. Limnology and Oceanography 41:1758–1766.

Franks, P. J. S. 2002. NPZ models of plankton dynamics: their construction, coupling to physics, and application. Journal of Oceanography 58:379–387.

Hansen, P. J., P. K. Bjornsen, and B. W. Hansen. 1997. Zooplankton grazing and growth: scaling within the 2–2,000 μm body size range. Limnology and Oceanography 42:687–704.

Hanson, P. C., T. B. Johnson, D. E. Schindler and J. F. Kitchell. 1997. Bioenergetics model 3.0 for Windows. Technical Report WISCU-T-97-001. Sea Grant Institute, University of Wisconsin, Madison.

Holt, D.D. 2004. Implications of system openness for local community structure and ecosystem function. Pages 96–114 *in* G. A. Polis, M. E. Power, and G. R. Huxel, eds. Food webs at the landscape level. University of Chicago Press, Chicago.

Jager, H. I., J. A. Chandler, K. B. Lepla, and W. Van Winkle. 2001. A theoretical study of river fragmentation by dams and its effect on white sturgeon populations. Environmental Biology of Fishes 60:347–361.

Jassby, A. D., J. E. Cloern, and B. E. Cole. 2002. Annual primary production: patterns and mechanisms of change in a nutrient-rich tidal ecosystem. Limnology and Oceanography 47:698–712.

Köhler, P., J. Chave, B. Riéra, and A. Huth. 2003. Simulating the long-term response of tropical wet forests to fragmentation. Ecosystems 6:114–128.

Larmola, T., J. Alm, S. Juutinen, S. Saarnio, P. J. Martikainen, and J. Silvola. 2004. Floods can cause large interannual differences in littoral net ecosystem productivity. Limnology and Oceanography 49:1896–1906.

Lopez, C. B., J. E. Cloern, T. S. Schraga, A. J. Little, L. V. Lucas, J. K. Thompson, and J. R. Burau. 2006. Ecological values of shallow-water habitats: implications for restoration of a disturbed ecosystem. Ecosystems 9:422–440.

Lovett, G. M., C. G. Jones, M. G. Turner, and K. C. Weathers, eds. 2005. Ecosystem function in heterogeneous landscapes. Springer, New York.

Müller-Solger, A. B., A. D. Jassby, and D. C. Müller-Navarra. 2002. Nutritional quality of food resources for zooplankton (*Daphnia*) in a tidal freshwater system (Sacramento–San Joaquin River Delta). Limnology and Oceanography 47:774–777.

Murray, A., and J. Parslow. 1997. Port Philip Bay integrated model: final report. Technical Report 44. Commonwealth Scientific and Industrial Research Organization Environmental Projects Office, Canberra, Australia.

Nichols, F. H., J. E. Cloern, S. N. Luoma, and D. H. Peterson. 1986. The modification of an estuary. Science 231:567–573.

Paetzold, A., C. J. Schubert, and K. Tockner. 2005. Aquatic terrestrial linkages along a braided river: riparian arthropods feeding on aquatic insects. Ecosystems 8:748–759.

Polis, G. A., W. B. Anderson, and R. D. Holt. 1997. Toward an integration of landscape and food web ecology: the dynamics of spatially subsidized food webs. Annual Review of Ecology and Systematics. 28:289–316.

Polis, G. A., M. E. Power, and G. R. Huxel, eds. 2004. Food webs at the landscape level. University of Chicago Press, Chicago.

Power, M. E., W. E. Rainey, M. S. Parker, J. L. Sabo, A. Smyth, S. Khandwala, J. C. Finlay, F. C. McNeely, K. Marsee, and C. Anderson. 2004. River-to-watershed subsidies in an old-growth conifer forest. Pages 217–240 *in* G. A. Polis, M. E. Power, and G. R. Huxel, eds. Food webs at the landscape level. University of Chicago Press, Chicago.

Pringle, C. 2003. What is hydrologic connectivity and why is it ecologically important? Hydrological Processes 17:2685–2689.

Reiners, W. A., and K. L. Driese. 2001. The propagation of ecological influences through heterogeneous environmental space. BioScience 51:939–950.

Reynolds, C. S. 2000. Hydroecology of river plankton: the role of variability in channel flow. Hydrological Processes 14:3119–3132.

Roberts, C. M. 1997 Connectivity and management of Caribbean coral reefs. Science 278:1454–1457.

Ross, A. H., W. S. C. Gurney, M. R. Heath, S. J. Hay, and E. W. Henderson. 1993. A strategic simulation model of a fjord ecosystem. Limnology and Oceanography 38:128–153.

Roughgarden, J., S. Gaines, and H. Possingham. 1988. Recruitment dynamics in complex life cycles. Science 241:1460–1466.

Sobczak W. V., J. E. Cloern, A. D. Jassby, and A. B. Müller-Solger. 2002. Bioavailability of organic matter in a highly disturbed estuary: the role of detrital and algal resources. Proceedings of the National Academy of Sciences of the USA 99:8101–8105.

Sommer, T., B. Harrell, M. Nobriga, R. Brown, P. Moyle, W. Kimmerer, and L. Schemel. 2001. California's Yolo Bypass: evidence that flood control can be compatible with fisheries, wetlands, wildlife, and agriculture. Fisheries 26:6–11.

Steele, J. H., and E. W. Henderson. 1992. The role of predation in plankton models. Journal of Plankton Research 14:157–172.

Tett, P. 1990. The photic zone. Pages 59–87 *in* P. J. Herring, A. K. Campbell, M. Whitfield, and L. Maddock, eds. Light and life in the sea. Cambridge University Press, Cambridge.

Tett, P., A. Edwards, and J. Jones. 1986. A model for the growth of shelf-sea phytoplankton in summer. Estuarine, Coastal and Shelf Science 23:641–672.

Thompson, J. N., O. J. Reichman, P. J. Morin, G. A. Polis, M. E. Power, R. W. Sterner, C. A. Couch, et al. 2001. Frontiers of ecology. BioScience 51:15–24.

Tockner, K., F. Malard, and J. V. Ward. 2000. An extension of the flood pulse concept. Hydrological Processes 14:2861–2883.

Troost, T. A., B. W. Kooi, and S. A. L. M. Kooijman. 2005. Ecological specialization of mixotrophic plankton in a mixed water column. American Naturalist 166:E45–E61.

Wofsy, S. C. 1983. A simple model to predict extinction coefficients and phytoplankton biomass in eutrophic waters. Limnology and Oceanography 28:1144–1155.

Associate Editor: James P. Grover
Editor: Donald L. DeAngelis